Meteorological drought analysis using copula theory for the case of upper Tekeze river basin, Northern Ethiopia

Biniyam Yisehak (b1n1y21@gmail.com)
Mekelle University https://orcid.org/0000-0002-9954-4344
Henok Shiferaw
Mekelle University
Atkilt Girma
Mekelle University
Zenebe Girmay
Mekelle University
Rahwa Kidane
Mekelle University

Research Article

Keywords: Copula theory, MSDI, Multivariate standardized drought, Mann-Kendall's trend test, Meteorological drought

Posted Date: September 10th, 2021

DOI: https://doi.org/10.21203/rs.3.rs-873511/v1

Version of Record: A version of this preprint was published at Theoretical and Applied Climatology on May 4th, 2022. See the published version at https://doi.org/10.1007/s00704-022-04061-0.

Abstract

Meteorological drought is a climate-related natural disaster. It indicates a shortage of precipitation over a long period, usually for a season or a year. This study was initiated to analyze meteorological drought using copula theory. Long-year (1982–2020) rainfall and soil moisture data were used to analyze standardized precipitation index (SPI) and standardized soil moisture index (SSI), respectively. The best-fit copula family was selected to construct the joint probability distribution (JPD) of SPI and SSI. Multivariate standardized drought index (MSDI) at 3-, 6-, and 12-month timescales were analyzed using the MSDI toolbox. The non-parametric Mann-Kendall (M-K) statistical test was used for trend detection. The result shows the newly developed MSDI captured all extreme drought events with the highest severity (-3.21) that occurred during the observation period compared to SPI and SSI. MSDI shows the famine caused by the drought of 1984 and 1985 remains well known to the world, with the drought duration and severity of 10 months and 18.7 years, respectively and its joint return period was 33.0 years. The result of the M-K and Sen's Slope estimator statistical tests shows a positive trend for all drought timescales in the basin. The extreme drought captured by the MSDI most frequently occurred in the basin. This implicated that meteorological drought analysis using multiple indices is better than a single index. The results of this study will help devise drought adaptation and mitigation strategies in the basin and beyond.

1. Introduction

On a global scale, meteorological drought has increased in recent decades, but this trend is more pronounced in the arid and semi-arid regions (Dai 2011; Saadat et al. 2013). Drought hazard is a recurrent extreme climate event with an enormous impact on human lives and the environment. Historically, drought-driven disasters are known to affect more people across the globe than any other disaster (Wilhite and Vanyarkho 2000). Therefore, in meteorological drought analysis, it is necessary to consider its multivariate nature and spatial variability explicitly.

In Ethiopia, drought (due to shortage of rainfall) is a recurrent event and induces serious challenges to crop production. It is also one of the natural hazards explained by a substantial reduction in rainfall availability for a prolonged period over a given region (Sousa et al. 2011). In northern Ethiopia, for instance, drought has been widely reported as one of the main natural disasters throughout human history (Gebrehiwot et al. 2011). As a result, food insecurity and environmental degradation were commonly reported, particularly in the arid and semi-arid parts of Northern Ethiopia (Ching et al. 2011; Nicholson 2000).

In Ethiopia, several studies were undertaken on meteorological drought and related issues. However, most of these studies used a single drought index to characterize the drought events. For example, Gidey et al. (2018) and Mohammed et al. (2018) used standardized precipitation index (SPI) to predict future meteorological drought hazards in Raya, Southern Tigray, and for meteorological drought assessment in Northeast highlands of Ethiopia, respectively. Similarly, Eze et al. (2020) also used this index to analyze yield reduction in recent drought years in Southern Tigray, Northern Ethiopia.

Drought characterization based on a single index has its limitation; for example, previous studies showed that the SPI is more likely to detect the onset of drought conditions, whereas drought persistence more effectively can be identified based on standardized soil moisture index (SSI) (Hao and AghaKouchak 2013). Hence, drought events are associated with multiple parameters (e.g., precipitation, soil moisture, and surface runoff), it is crucial to undertake multivariate analysis considering multiple parameters when assessing and characterizing the drought events. The outcomes of the multivariate drought characterization are important for assessing its potential risks (Shiau 2006).

Drought characteristics may have different marginal distribution functions, the most suitable tool for achieving the joint behavior of the drought characteristics in multivariate copula functions. Moreover, the benefit of using Copula functions is the possibility of using different univariate marginal distributions (Vaziri et al. 2018). Copula functions as a

multivariate analysis method are widely used to analyze the functional structure of drought characteristics (Chen et al. 2013; Hao et al. 2017; Mirakbari et al. 2010). Thus, meteorological drought analysis using copula theory, provides a promising opportunity to deal with such risks in advance and to improve sectorial resilience.

Thus, this study aims to analyze meteorological drought using copula theory. Specifically, the study focuses on analyzing the (i) temporal variation of meteorological drought at three different timescales (3-month, 6-month, and 12-month), (ii) meteorological drought return period at 3-month timescale, (iii) long-term trends of meteorological drought, and (iv) mapping the spatial extent of meteorological drought severity at 3-month timescale.

2. Materials And Methods

2.1. Description of the study area

The study area Upper Tekeze River Basin (UTRB), is located between $11^\circ 40'$ to $14^\circ 32'$ N and $36^\circ 30'$ to $39^\circ 50'$ E with a basin area of 43,000km^2 (Fig. 1). The altitude of the study area ranges between 828 and 4,517 m.a.s.l. This elevation difference has a high potential for hydropower production in the mountainous areas and irrigation lands in the lowlands. The climate of UTRB varies depending on location. The temperature varies from 3 to 21 ℃ and 19 to 43 ℃ in the highland and lowland areas, respectively. The annual rainfall varies from 600 to 1,300 mm from the lowland usually highland areas. Three seasons can be recognized in UTRB namely: i) the dry (Bega) (from October to January); ii) small rain (Belg) (from February to May), and iii) wet (Kiremt) from (June to September). The main soils of UTRB are Eutric Cambisols, Calcric Cambisols, and Euric Vertisols (FAO 2002). The land use and land cover of the basin include agricultural land (64%), shrubland (range grasses) (15%), mixed forests (12%), and pasture/grazing lands (9%). The main crops grown in the basin are teff, wheat, barley, and maize (Fentaw et al. 2018).

2.2. Data and Data Sources

In this study, long-year monthly time series observed rainfall data for the period 1982–2020 was collected from 12 meteorological stations (Mekelle, Maichew, Axum, Gonder, Shire, Adigudem, Hawzen, Hagere/Selam, Debre/Tabor, Lalibela, Wukro, and Debarik) which are found in and around the UTRB (Fig. 1; Table.1). Rainfall data were obtained from the National Meteorological Agency of Ethiopia (NMA). Monthly 0.25° spatial resolution harmonized satellite-derived soil moisture data for the same period of rainfall was downloaded from European Space Agency (ESA) Climate Change Initiative (CCI) dataset.

2.3. Meteorological data gap filling

Filling of missed value is not recommended to avoid errors, since it may lead to the wrong conclusions. Therefore, the first step for data analysis should be station selection based on their data quality and length of years of records. The percentage of missing rainfall data was calculated for each of the stations. Several rain gauge stations had incomplete records. To make use of the partially recorded data, missing values need to be filled in sequence. Various approaches are available to fill the missing recorded rainfall gauging data. In this study, the missing values were filled with the delta change approach R-program Girma (2017) using Climate Hazards Group Infrared Precipitation Stations (CHIRPS) satellite data. It was preferred because it has a relatively high resolution and it is commonly used in Africa (Katsanos et al. 2016; Shukla et al. 2014). According to Gebremicael et al. (2017) CHIRPS rainfall data showed a good correlation with observed rainfall in UTRB.

Table 1
General information on rainfall stations, latitude and longitude, altitude (Alt.) in meters above sea level (m a.s.l.), mean annual rainfall (mm yr − 1), Standard deviation (SD) (mm yr − 1), Coefficient of variation (CV), and percentage of missing data

SN	Station name	Lat. (∘)	Long. (∘)	Alt. (m)	Recording period	Analysis period	Mean (%)	SD	CV (%)	Missing Data (%)
1	Mekelle	13.45	39.53	2260	1952–2020	1982–2020	616	144	23	9.5
2	Maichew	12.69	39.54	2432	1953–2020	1982–2020	735	135	18	11.7
3	Axum	14.12	38.74	2200	1962–2020	1982–2020	774	110	14	9.4
4	Gonder	12.60	37.50	2316	1952–2020	1982–2020	1173	119	10	6.3
5	Shire	14.10	38.28	1920	1963–2020	1982–2020	893	106	12	10.1
6	Adigudem	13.16	39.13	2100	1975–2020	1982–2020	659	115	17	12.1
7	Hawzen	13.98	39.43	2255	1971–2020	1982–2020	575	89	16	6.6
8	H/Selam	13.65	39.17	2630	1973–2020	1982–2020	721	123	17	13.6
9	D/tabor	11.85	38.00	2969	1974–2020	1982–2020	1529	174	11	2.3
10	Lalibela	12.03	39.05	2450	1972–2020	1982–2020	875	144	16	5.3
11	Wukro	13.79	39.60	1995	1962–2020	1982–2020	558	105	19	9.4
12	Debarik	13.15	37.90	2850	1955–2020	1982–2020	1174	116	10	6.2

2.4. Temporal variation of meteorological drought

Long-year monthly rainfall and soil moisture data were used to analyze standardized precipitation index (SPI) and standardized soil moisture index (SSI), respectively. In this study, the gamma distribution function (GDF) was used to analyze both SPI and SSI, the GDF defined by Thom (1966) as follows:

$$g(x) = \frac{1}{\beta^{\alpha}\Gamma(\alpha)} x^{\alpha-1} e^{-x/\beta} \quad (7)$$

Where α and β are the shape and scale parameters respectively, Γ is an ordinary GDF. These α and β parameters were determined following Thom (1966) and Edwards (1997). The cumulative distribution function (CDF) of GDF was estimated by:

$$G(x) = \int_0^x g(x)\,dt (8)$$

To overcome the restriction of GDF to fit time series with zero values, Thom (1951) presented mix distribution function as follows:

$$H(x) = q + (1 - q)\,G(x) (9)$$

In the above equation, the probability of zero is estimated as, $q = m/n$ where m and n are the number of zero values and the sample number of time series respectively. Finally, the GDF is normalized using the procedure described by Hastings (1955) and Abramowitz and Stegun (1965) to estimate SPI or SSI. A positive SPI or SSI value corresponds to the wet condition. A negative SPI refers to a precipitation value less than below normal conditions and a negative SSI refers to a soil moisture value less than below normal conditions and is defined as drought period (Table 2).

Table 2
Climatic moisture categories for the SPI and SSI (Shekhar & Shapiro 2019)

SN	Climatic moisture categories	SPI/SSI
1	Extremely wet	≥ 2.0
2	Severely wet	$1.5 to 1.99$
3	Moderately wet	$1.0 to 1.49$
4	Normal	$0.99 to -0.99$
5	Moderately drought	$-1.0 to -1.49$
6	Severely drought	$-1.5 to -1.99$
7	Extremely drought	≤ -2.0

2.5. Copula theory

The copula family is commonly adopted to combine standard uniform probabilities to their subsequently join probability distributions (JPDs) and the dependence structure of randomly distributed dependent variables. This concept comes into existence to overcome the limitations associated with conventional multivariate frequency distributions. The conventional multivariate distributions are not explicitly expressed in terms of their corresponding marginal probabilities, whereas copula theory is associated with Sklar (1959) theorem. As per this theorem, the joint distribution function of the marginal distribution function of two continuous random variables X and Y can be represented by:

$$F(x, y) = C[F(x), G(y) = C(u, v) (4)$$

where $F(X)$ and $G(Y)$ are marginal probability distributions and C is a mapping function popularly known as a copula, which performs the joining of two marginal probability distributions.

The $C(u, v)$ is a bivariate copula and involves marginal variables. A detailed conceptualization of copula theory is depicted in Fig. 2 (Favre et al. 2004).

In this study, Gaussian, t, Clayton, Frank, and Gumbel copula families were considered to construct the JPD of the two variables, and the best-fit represented copula is adopted for final assessment. Table.3 shows the relationships between five different copula families and parameter ranges.

Table 3 Relationships of five different copula functions and parameter ranges

SN	Name	Copula equation	Parameter range	Reference
1	Gaussian	$\int_{-\infty}^{\phi^{-1}(u)}\int_{-\infty}^{\phi^{-1}(v)}\frac{1}{2\pi\sqrt{1-\theta^2}}exp\left(\frac{2\theta xy-x^2-y^2}{2(1-\theta^2)}\right)dxdy^b$	$\theta \in [-1,1]$	(C. Li et al., 2013)
2	t	$\int_{-\infty}^{t_{\theta_2}^{-1}(u)}\int_{-\infty}^{t_{\theta_2}^{-1}(v)}\frac{\Gamma((\theta_2-2)/2)}{\Gamma(\theta_2/2)2\pi\sqrt{1-\theta_1^2}}\left(1+\frac{x^2 2\theta_1 xy+y^2}{\theta_2}\right)^{(\theta_2-2)/2}dxdy^c$	$\theta_1 \in [-1,1]$ and $\theta_2 \in (0,\infty)$	(C. Li et al., 2013)
3	Clayton	$C(u,v)=\max(u^{-\theta}+v^{-\theta}-1,0)^{-1/\theta}$	$\theta \in [-1,\infty)\backslash 0$	(Clayton, 1978)
4	Frank	$-\frac{1}{\theta}\ln\left[1+\frac{(exp(-\theta u)-)(exp(-\theta v)-)}{exp(-\theta)-1}\right]$	$\theta \in \mathbb{R}\backslash 0$	(C. Li et al., 2013)
5	Gumbel	$exp\left\{-\left[(-\ln(u))^{\theta}+(-\ln(v))^{\theta}\right]^{1/\theta}\right\}$	$\theta \in [1,\infty)$	(C. Li et al., 2013)

2.6. Goodness-of-fit tests

To develop the joint probability distribution (JPD) of both SPI and SSI, it is very important to select the best-fit copula family. The multivariate copula analysis toolbox (MvCAT) by Sadegh et al. (2017) in MATLAB was adopted for carrying out the goodness-of-fit tests. MvCAT includes both the commonly used local optimization method and state-of-the-art Markov Chain Monte Carlo (MCMC) framework. In this study, the Max-Likelihood value, Akaike Information Criterion (AIC), Bayesian Information Criterion (BIC), root mean square error (RMSE), and Nash-Sutcliff efficiency (NSE) were used to evaluate the performance of the different copula families. A parameter set that gives the maximum likelihood reduces the residuals between model simulations and observations. It, therefore, gives, in this sense, the best fit to the observed data (Sadegh et al. 2017). Higher model complexity offers the benefit of better model suppleness and hereafter mostly outcomes in the best fit to the actual data. Though, this strength rouse from the excess of the model. AIC, in comparison with advertising opportunity value, considers both the complication of the model and reduction of error and offers an extra rigorous measure of the excellence of model estimation. AIC removes the problem from excess by accessing a mulct term grounded on the number of parameters. AIC is developed by Aho et al. (2014) and Akaike (1974), and is calculated as:-

$$AIC = 2D - 2l, \quad (1)$$

Where D is the number of parameters of the model and l is the value of the best parameter of copula function. This formula can be used to give an estimate of Gaussia error residues, $\left(\begin{matrix}-2\\ \sigma\end{matrix} = \frac{\sum_{i=1}^{n}\left[\tilde{y}_i - y_i(\theta)\right]^2}{n}\right)$

$$AIC = 2D + n\ln\left\{\frac{\sum_{i=1}^{n}\left[\tilde{y}_i - y_i(\theta)\right]^2}{n}\right\} - 2l, \quad (2)$$

Where $\tilde{y}_i$ is computed parametric copula function, {y}_{i}\left(\theta \right) is the likelihood of observed data from empirical copula function, and n is the total number of observations

A minimum AIC value corresponds to a better model. likely to AIC, BIC is explained by Schwarz (1978).

BIC=D\text{ln}n-2l \left(3\right)
which similarly simplifies to

BIC=D\text{ln}n+n\text{ln}\left\{\frac{\sum _{i=1}^{n}{\left[{\tilde{y}}_{i}-{y}_{i}\left(\theta \right)\right]}^{2}}{n}\right\}-2l, \left(4\right)
If the Gaussian distribution is centered around zero, the residuals are independent and evenly distributed. Likely to AIC, a minimum BIC value related with a better model fit.

NSE is developed by Nash & Sutcliffe (1970) and RMSE are also two extensively used measures of goodness of fit, which only emphasize on reduction of error,

RMSE=\sqrt{\frac{\sum _{i=1}^{n}{\left[{\tilde{y}}_{i}-{y}_{i}\left(\theta \right)\right]}^{2}}{n}} \left(5\right)
NSE=1-\frac{\sum _{i=1}^{n}{\left[{\tilde{y}}_{i}-{y}_{i}\left(\theta \right)\right]}^{2}}{\sum _{i=1}^{n}{\left[{\tilde{y}}_{i}-{\stackrel{-}{\tilde{y}}}_{i}\right]}^{2}} \left(6\right)
A best-fit model is related with RMSE=0,RMSE\in \left[0,\left.\infty \right)\right.,and NSE=1, NSE\in \left(-\infty ,\left.1\right]\right.. Although several copula parameters impact some evaluation metrics, parameter ranges have no impact on them.

2.7. Multivariate standardized drought index (MSDI)

To address the limitations associated with the univariate drought index for meteorological drought characterization, a copula-based multivariate standardized drought index is advocated that integrates the advantage of univariate drought indices and is expressed as

$$P = P(SPI < x, SSI < y) = C[F(SPI), G(SSI)] \quad (7)$$

Where P is the joint probability of two indices, C is the copula member for constructing the joint probability distribution (JPD), and F\left(SPI\right) and G\left(SSI\right) are marginal cumulative distribution functions of SPI and SSI, respectively.

The best-fit copula was selected to construct the joint probability distribution using their respective generator function. Finally, MSDI was derived from the joint probability distribution of SPI and SSI. MSDI at 3-, 6-, and 12-month time scales were computed to examine the characteristics of meteorological drought in short-term, medium-term, and long-term periods. The transformation function is given as follows:

MSDI={\Phi }^{-1}\left(P\right) \left(8\right)
Where {\Phi } is the transformation function that converts the JPD into the same scale and space as that of the SPI and SSI to assess the performances of both the indices on a single platform.

2.8. Multivariate return period

Multivariate return period, which considers both drought duration and severity, can be divided into the probability of exceeding both drought duration and severity (D>d and S>s), or the probability of exceeding either drought duration or severity (D>d or S>s). For each condition, the copulas-based return period can be defined as follows:

{T}_{\left(DS\right)}=\frac{E\left(L\right)}{1-{F}_{D}\left(d\right)-{F}_{S}\left(s\right)+C({F}_{D}\left(d\right), {F}_{S}\left(s\right))} \left(9\right)
{{T}^{,}}_{\left(DS\right)}=\frac{E\left(L\right)}{1-C({F}_{D}\left(d\right),{F}_{S}\left(s\right))} \left(10\right)
Where {T}_{\left(DS\right)}and {{T}^{,}}_{\left(DS\right)} are the joint return period for (D>d and S>s) and (D>d or S>s), respectively. E\left(L\right) is the mean interval time between the drought events. {F}_{D}\left(d\right) and {F}_{S}\left(s\right) are the cumulative distributions of drought duration and severity, respectively.

2.9. Meteorological drought trend analysis

The non-parametric Mann-Kendall statistical test (Kendall 1975; Mann 1945) was used for trend detection, due to its sturdiness for non-normally distributed functions, which are frequently encountered in hydroclimatic time series data (Gao et al. 2011; Zhao et al. 2016). The test has been commonly recommended by WMO (2009). The test statistical algorithm can be given as

S=\sum _{i=1}^{n}\sum _{j=1}^{i-1}sign\left({x}_{i}-{x}_{j}\right) \left(11\right)
Where, n is the total length of data, {x}_{i} and {x}_{j} are two generic sequential data values, and function sign({x}_{i}-{x}_{j}) assumes the following values

$$sign(x_i - x_j) = \begin{bmatrix} 1, if\ (x_i - x_j) > 0 \\ 0, if\ (x_i - x_j) = 0 \\ -1, if\ (x_i - x_j) < 0 \end{bmatrix} \quad (12)$$

Under this test, the statistics S is approximately normally distributed with the mean E\left(S\right) and the variance Var\left(S\right) can be computed as follow:

E\left(S\right)=0 \left(13\right)
Var\left(S\right)=\frac{1}{n}\left[n\left(n-1\right)\left(2n+5\right)-\sum _{t}t(t-1)(2t+5)\right] \left(14\right)
Where n is the length of time series, and t is the extent of any given tie and \sum t denotes the summation over all tie number of values. The standardized Z for this test can be calculated by the following equation:

$$Z = \begin{bmatrix} \frac{S+1}{\sqrt{Var(S)}}, if\ S > 0 \\ 0, if\ S = 0 \\ -1, if\ S < 0 \end{bmatrix} \quad (15)$$

The null hypothesis {H}_{o} is accepted, if a data set of n independent randomly distributed variables have no trend with equally likely ordering. Any Z>0 indicates a rising, while Zcript> may conclude a declining trend in series.

2.10. The spatial extent of meteorological drought severity

The inverse distance weighted (IDW) method has been used to map the spatial extent of standardized precipitation index (SPI), standardized soil moisture index (SSI), and multivariate standardized drought index (MSDI) at a 3-month scale. IDW is intuitive and efficient for spatial analysis (Shepard 1968). The analysis was done using the geostatistical analysis tool of Arc Map 10.2. The IDW technique computes an average value for unsampled locations using values nearby weighted locations. The weights are proportional to the proximity of the sampled points to the unsampled location and can be specified by the IDW power coefficient. The larger the power coefficient, the stronger weight of nearby points as can be gleaned from the following equations that estimate the value {Z}_{j} at an unsampled location j.

{Z}_{j}=\frac{{\sum }_{i}{Z}_{i}/{d}_{ij}^{n}}{\sum _{i}1/{d}_{ij}^{n}} \left(16\right)
Where {Z}_{j} is the estimated value, n is the weighted parameter, d is the nearest distance

3. Result And Discussion

3.1. Best-fit-copula family

This study is limited to evaluate the effects of precipitation and soil moisture where the standardized precipitation index (SPI) and standardized soil moisture index (SSI) were joined to model the multivariate standardized drought index (MSDI). Among all copula families, the Gumbel copula was selected as the best-fit distribution for 3- and 6-month drought timescales, while the Frank copula was the best-fit distribution for 12-month drought timescale. The joint probability distribution (JPD) of SPI and SSI was constructed based on all goodness-of-fit criteria (Max-Likelihood, AIC, BIC, NSE, and RMSE), which is in agreement with the finding of (Dash et al. 2019; Ghafori et al. 2019; Zhang et al. 2015). Therefore, the

MSDI was constructed by using the Gumbel and Frank copula. The goodness-of-fit tests for 3-, 6-, and 12-month drought timescales are shown on Table.4. The detailed description of empirical and fitted probability, the dependent structure of SPI and SSI, and posterior distribution of the copula family are presented in Fig. 3–5.

Table 4
The goodness-of-fit tests assessment of copula family (Gaussian, t, Clayton, Frank, and Gumbel) for 3-, 6-, and 12-month drought timescales in the Upper Tekeze River Basin

Drought timescales	Copula Family	NSE	RMSE	AIC (Rank)	BIC (Rank)	Max-Likelihood	Best-fit
3-month	Gaussian	0.9982	0.2352	2	2	2	
	t	0.9979	0.2378	3	3	3	
	Clayton	0.9968	0.2940	5	5	5	
	Frank	0.9977	0.2468	4	4	4	
	Gumbel	0.9982	0.2176	1	1	1	
6-month	Gaussian	0.9979	0.2382	3	3	3	
	t	0.9978	0.2429	4	4	4	
	Clayton	0.9967	0.2951	5	5	5	
	Frank	0.9979	0.2377	2	2	2	
	Gumbel	0.9980	0.2327	1	1	1	
12-month	Gaussian	0.9968	0.2903	2	2	2	
	t	0.9968	0.2942	3	3	3	
	Clayton	0.9950	0.3638	5	5	5	
	Frank	0.9969	0.2862	1	1	1	
	Gumbel	0.9967	0.2952	4	4	4	

3.2. Temporal variation of meteorological drought

The results of the monthly temporal variation of SPI, SSI, and MSDI were analyzed using a 3-, 6-, and 12-month drought timescales in the Upper Tekeze River Basin during the period 1982 to 2020, and the results are depicted on Fig. 6. The drought pattern of SPI and SSI are not similar, there are some inconsistencies between the two indices. SPI shows that the drought onset several months earlier than SSI. Moreover, SPI drought onset is similar to a newly developed MSDI. However, the SSI shows that the drought persistence is similar to that of MSDI. For example, from Dec-1982 to Jul-1983 SPI-12 showed dry, while SSI-12 showed continuously wet until Mar-1985. SSI has a delayed response to the SPI under dry soil conditions, whereas for wet soil conditions the quick response of the SSI to the SPI is dominant (Kwon et al. 2019).

SPI and SSI captured different extreme drought years, for example, the SPI captured maximum drought severity (-2.17) in the years 1984, 1985, 1988, and 1991, while SSI captured in the years 2004 and 2005, with similar drought severity of SPI. MSDI captured all extreme drought events with the highest magnitude that occurred from 1982 to 2020 and more similarly, captured the extreme drought events detected by SPI. The precipitation-based SPI drought is more variable than

SSI (Fig. 6). Both SPI and SSI show significant variation in terms of severity and duration (Dash et al. 2019; Z. Hao and AghaKouchak 2013; Kwon et al. 2019). Detailed analysis indicated that SPI captures the drought earlier than SSI for the concerned period and it exhibits a greater degree of variability than SSI. MSDI would perform better than SPI and SSI (Dash et al. 2019; Yisehak and Zenebe 2020).

3.3. Meteorological drought return period

The return period of drought events is usually related to a certain exceedance probability. Unlike the flood frequency analysis, a specific drought event may happen multiple times in 1-year and may also continue for several months (Ghafori et al. 2019). Then, a drought characteristic, average drought interval time, is required for estimating the return period of drought duration and severity. The average drought interval time was, thus, calculated using the best-fit copula function. The average interval time between the 3-month timescale of drought events was estimated to be 1.7, 3.9, and 4.0 months for SPI, SSI, and MSDI, respectively. The contour lines were used to represent the joint return period of severity and duration. Figure 7 shows the joint return period of severity and duration of drought according to Eq. 10.

Identifying the joint return periods of drought duration and severity is vital for meteorological drought monitoring, water resources management, and hydraulic design criterion and provides useful information for evaluating risk (Shiau 2006; Song and Singh 2010). The values of dependent drought duration and severity for the multivariate return periods 2, 5, 10, 20, 50, 100, 200, and 500 years are presented in Fig. 7. The famine caused by the drought of 1984 and 1985 remains well known to the world community (Edossa et al. 2010), with the drought duration and severity of 7 months and 11.7, respectively. The joint return period for a drought duration of 7 months or a drought severity of 11.7 was greater than 500 years return period. In the above historical drought years, the MSDI showed that the joint return period for a drought duration of 10 months or a drought severity of 18.7 was 33.0 years. Both SPI and MSDI show the shortest and the most severe recent meteorological drought event in the basin which occurred during the year 2015, with the drought duration of 3 month and severity of 5.0. The joint return period for a drought duration of 3 months or a drought severity of 5.0 was 14.2 and 1.8 years for SPI and MSDI, respectively (Fig. 7a and e).

3.4. Long-term trends of meteorological drought

A simulations assessment of drought trends using multivariate drought indices is useful for drought planning and management (Temam et al. 2019). The result of the Mann-Kendall (M-K) and Sen's Slope estimator statistical tests for SPI, SSI, and MSDI at multiple timescales for 12 meteorological stations over the UTRB for the period 1982 to 2020 are presented in Table 5–7. The P-value in bold illustrates a statistically insignificant trend of drought. The positive and negative values of Z statistics show the wetting and drying trend, respectively.

For all drought timescales, SPI detects a positive trend for Mekelle, Maichew, Axum, Gonder, D/Tabor, Lalibela, Wukro, and Debarik stations, while, for Shire, Hawzen, and H/selam stations, it detected a negative trend. For Adigudem station the trend at the 5% significance level using 3- and 6-month drought timescales had insignificant trend (Table 5). Also, SSI detects insignificant trend using the 3-month drought timescale for Mekelle, Adigudem, Hawzen, and Wukro stations. However, for all drought timescales for Shire and H/Selam stations, it detected a negative trend. SSI detects a positive trend using 3-, 6-, and 12-month for Maichew, Axum, Gondar, D / Tabor, Lalibela and Debark stations (Table 6).

Newly developed MSDI for 12-month drought timescales detects a positive and negative trend at all stations, except Adigudem (Table 7). In general, M-K and Sen's Slope estimator statistical tests result shows a positive trend for all drought timescales over the UTRB (Table 5–7). In the northeast part of the basin, the rainfall trend significantly decreased, whereas there is an increasing tendency in the southwest part of the basin (Gebremicael et al. 2017). According to Temam et al. (2019) in the northeast part of the Ethiopia show a negative trend (decline in rainfall trend) of meteorological drought.

Table 5

Result of Mann-Kendall's trend and Sen's Slope for 3-month, 6-month, and 12-month SPI, p-value less than 0.05 at the 5% significance level during 1982–2020 for 12 stations and Upper Tekeze River Basin (UTRB) Northern Ethiopia

SN	Station	SPI-3			SPI-6			SPI-12		
		Kendall's tau	Sen's Slope	p-value	Kendall's tau	Sen's Slope	p-value	Kendall's tau	Sen's Slope	p-value
1	Mekelle	0.107	0.014	0.001	0.163	0.022	0.001	0.200	0.029	0.001
2	Maichew	0.082	0.011	0.008	0.123	0.017	0.001	0.143	0.021	0.001
3	Axum	0.980	0.130	0.002	0.610	0.220	0.001	0.750	0.250	0.001
4	Gonder	0.146	0.020	0.001	0.216	0.029	0.001	0.279	0.038	0.001
5	Shire	-0.650	-0.080	0.037	-0.216	-0.150	0.000	-0.211	-0.160	0.000
6	Adigudem	0.003	0.000	**0.932**	0.048	0.006	**0.123**	0.058	0.009	0.042
7	Hawzen	-0.074	-0.009	0.018	-0.098	-0.013	0.002	-0.073	-0.010	0.020
8	H/Selam	-0.106	-0.014	0.001	-0.176	-0.024	0.001	-0.188	-0.028	0.001
9	D/Tabor	0.151	0.020	0.001	0.191	0.026	0.001	0.232	0.320	0.001
10	Lalibela	0.107	0.014	0.001	0.152	0.021	0.001	0.197	0.029	0.001
11	Wukro	0.094	0.012	0.002	0.143	0.019	0.001	0.145	0.020	0.001
12	Debarik	0.153	0.020	0.001	0.167	0.023	0.001	0.175	0.026	0.001
13	UTRB	0.116	0.016	0.001	0.163	0.023	0.023	0.186	0.026	0.001

Table 6
Result of Mann-Kendall's trend and Sen's Slope for 3-month, 6-month, and 12-month SSI, p-value less than 0.05 at the 5% significance level during 1982–2020 for 12 stations and Upper Tekeze River Basin (UTRB) Northern Ethiopia

SN	Station	SSI-3			SSI-6			SSI-12		
		Kendall's tau	Sen's Slope	p-value	Kendall's tau	Sen's Slope	p-value	Kendall's tau	Sen's Slope	p-value
1	Mekelle	0.055	0.014	**0.076**	0.069	0.008	0.027	0.111	0.013	0.000
2	Maichew	0.078	0.010	0.012	0.085	0.010	0.006	0.112	0.015	0.000
3	Axum	0.080	0.011	0.010	0.113	0.015	0.000	0.143	0.019	0.001
4	Gonder	0.169	0.023	0.001	0.198	0.028	0.001	0.259	0.035	0.001
5	Shire	-0.178	-0.024	0.001	-0.199	-0.027	0.001	-0.245	-0.032	0.001
6	Adigudem	-0.043	-0.004	**0.168**	-0.056	-0.005	**0.075**	-0.100	-0.011	0.001
7	Hawzen	0.051	0.007	**0.100**	-0.062	-0.008	0.046	-0.069	-0.009	0.027
8	H/Selam	-0.109	-0.013	0.000	-0.137	0.015	0.001	-0.163	-0.019	0.001
9	D/Tabor	0.121	0.016	0.001	0.130	0.017	0.001	0.191	0.023	0.001
10	Lalibela	0.088	0.011	0.005	1.000	1.000	0.001	0.126	0.016	0.001
11	Wukro	-0.059	-0.007	**0.058**	-0.060	-0.008	**0.056**	-0.071	0.011	0.024
12	Debarik	0.262	0.036	0.001	0.299	0.040	0.001	0.355	0.049	0.001
13	UTRB	0.131	0.018	0.001	0.151	0.021	0.001	0.193	0.027	0.001

Table 7
Result of Mann-Kendall's trend and Sen's Slope for 3-month, 6-month, and 12-month MSDI, p-value less than 0.05 at the 5% significance level during 1982–2020 for 12 stations and Upper Tekeze River Basin (UTRB) Northern Ethiopia

SN	Station	MSDI-3			MSDI-6			MSDI-12		
		Kendall's tau	Sen's Slope	p-value	Kendall's tau	Sen's Slope	p-value	Kendall's tau	Sen's Slope	p-value
1	Mekelle	0.011	0.000	**0.718**	0.060	0.001	**0.053**	0.091	0.001	0.004
2	Maichew	0.089	0.001	0.004	0.133	0.001	0.001	0.188	0.002	0.001
3	Axum	0.115	0.001	0.000	0.201	0.002	0.001	0.256	0.003	0.001
4	Gonder	0.214	0.002	0.001	0.276	0.003	0.001	0.362	0.004	0.001
5	Shire	-0.156	-0.002	0.001	-0.230	-0.002	0.001	-0.287	-0.003	0.001
6	Adigudem	-0.048	-0.001	**0.122**	-0.008	0.000	**0.786**	0.011	0.000	**0.733**
7	Hawzen	-0.077	-0.001	0.013	-0.115	0.001	0.000	-0.120	-0.001	0.000
8	H/Selam	-0.126	-0.001	0.001	-1.179	0.002	0.001	-0.225	-0.002	0.001
9	D/Tabor	0.199	0.002	0.001	0.249	0.002	0.001	0.298	0.003	0.001
10	Lalibela	0.113	0.001	0.000	0.156	0.002	0.001	0.206	0.002	0.001
11	Wukro	0.022	0.000	**0.484**	0.069	0.001	0.026	0.088	0.001	0.005
12	Debarik	0.267	0.003	0.001	0.319	0.003	0.001	0.388	0.004	0.001
13	UTRB	0.148	0.018	0.001	0.202	0.026	0.001	0.248	0.032	0.001

3.5. The spatial extent of meteorological drought severity

In this study, we examined drought coverage over the UTRB for a short-term (3-month) drought timescale based on the percentage occurrence of each drought category (extreme, moderate, and severe) for each station concerning a total number of observations over the basin in the same drought category. The purpose is to identify areas repeatedly hit by each drought category, based on the percentage of occurrence. Figure 8 shows the spatial extent of meteorological drought occurrences for SPI, SSI, and MSDI at a 3-month drought timescale and drought category over the Basin. It can be noted from the result that the percentage occurrence of a drought event of a given drought category varies with location and drought indices. The SSI was found to be more sensitive to drought assessment than SPI in characterizing the spatial difference of drought. Unlike this, previous studies reported that SSI at the 3-month timescale can serve as a good indicator of changes in drought coverage (Z. Hao and AghaKouchak 2013; Kao and Govindaraju 2010; Li et al. 2012).

The SPI and SSI show the most frequent extreme drought occurred in Lalibela and Mekelle stations, respectively (Fig. 8a and d), while MSDI shows the most frequent extreme drought occurred in Hawzen, Wukro, and Adigudem stations (Fig. 8g). The SPI and SSI show the most frequently severe drought occurred in Hagere Selam and Mekelle stations, while SSI shows in Maichew stations (Fig. 8b and e). The MSDI shows most frequently only in the Lalibela station (Fig. 8f). Both SPI and MSDI show in Maichew station, most frequently affected by moderate drought (Fig. 8c and i), while SSI shows in Gonder station (Fig. 8f). Generally, in the basin between 5 to 24% are covered by moderate drought. Indeed those areas were among the worst drought-affected areas in the history of Ethiopia which is in line with the previous findings (Bayissa et al. 2015; Gebrehiwot et al. 2011; Liou & Mulualem 2019).

4. Conclusions

Drought is one of the worst natural disasters, its trend and returns period analysis is very important from a water resource management perspective. Moreover, focusing on one aspect of drought, the multivariate nature of drought impact towards drought phenomenon will give a wide knowledge about the frequency and distribution of drought both temporal and spatial extent. Moreover, meteorological drought analyzes based on multiple drought indices are useful for reducing and mitigating the impacts of drought on water resources. The results from the MSDI can contribute to monitoring the onset and persistence of meteorological drought as an early warning system. In this study, the temporal and spatial extent of meteorological drought conditions, the MSDI captures more extreme drought events than SPI and SSI. This shows that MSDI can give more information than a single index.

In this study to analyze MSDI, the authors used the drought information from observed ground rainfall and satellite soil moisture data. It may give insufficient information because satellite data have more inaccuracy and cannot represent the exact location of ground stations in the basin. Therefore, for a better understanding of the multivariate nature of drought, the authors recommend to used observed soil moisture data. Moreover, in the future, we recommend the researchers evaluate the integrations between other indices rather than SPI and SSI. The result of MSDI will be useful for farmers and governmental and non-governmental organizations who working on agrometeorological drought in the decision-making process for crop planning, irrigation scheduling, and for policymakers to implement water resource management and planning in the basin.

Declarations

Acknowledgments The research presented was financially supported by Institute of Climate and Society, Mekelle University (General Junior Research Project). We acknowledge the National Meteorology Agency of Ethiopia for providing the ground rainfall data of our study area free of charge.

Author contributions All authors collaborated in the research presented in this publication by making the following contributions: conceptualization and model developing, BY, HS, AG; lead data collection and data analysis, BY, HS, AG, ZG, RK;writing oral draft preparation, BY; writing – review & editing, BY, HS, AG, ZG, and RK.

Funding This work was supported by Institute of Climate and Society (ICS), Mekelle University [grant number RDPDO/MU/CBE/GeneralJunior/050/13, 2021].

Data availability The data and material used in this research will be available upon request from the correponding author.

Ethical approval The authors paid attention to the ethical rules in the study. There is no violation of ethics.

Consent to participate Not applicable.

Consent for publication Not applicable.

Conflict of interests The authors have declared that there is no conflict of interests

References

Abramowitz, M., & Stegun, I. A. (1965). *Handbook of mathematical functions: with formulas, graphs, and mathematical tables 55 (Courier Corporation)* (M. A. and I. A. Stegun (ed.); 3rd ed.). National Bureau of Standards Applied Mathematics Series - 55. https://doi.org/64-60036

Aho, K., Derryberry, D., & Peterson, T. (2014). Model selection for ecologists: the worldviews of AIC and BIC. *Ecology*, *95*(3), 631–636. https://doi.org/https://doi.org/10.1890/13-1452.1

Akaike, H. (1974). A new look at the statistical model identification. In *Selected Papers of Hirotugu Akaike* (pp. 215–222). Springer.

Bayissa, Y. A., Moges, S. A., Xuan, Y., Van Andel, S. J., Maskey, S., Solomatine, D. P., Griensven, A. Van, & Tadesse, T. (2015). Spatio-temporal assessment of meteorological drought under the influence of varying record length: The case of Upper Blue Nile Basin, Ethiopia. *Hydrological Sciences Journal*, *60*(11), 1927–1942.

Chen, L., Singh, V. P., Guo, S., Mishra, A. K., & Guo, J. (2013). Drought analysis using copulas. *Journal of Hydrologic Engineering*, *18*(7), 797–808.

Ching, L., Edwards, S., & El-Hage, S. (2011). *Climate change and food systems resilience in sub-saharan Africa.* Food and Agriculture Organization of the United Nations (FAO).

Clayton, D. G. (1978). A model for association in bivariate life tables and its application in epidemiological studies of familial tendency in chronic disease incidence. *Biometrika*, *65*(1), 141–151.

Dai, A. (2011). Drought under global warming: a review. *Wiley Interdisciplinary Reviews: Climate Change*, *2*(1), 45–65.

Dash, S. S., Sahoo, B., & Raghuwanshi, N. S. (2019). A SWAT-Copula based approach for monitoring and assessment of drought propagation in an irrigation command. *Ecological Engineering*, *127*, 417–430. https://doi.org/https://doi.org/10.1016/j.ecoleng.2018.11.021

Edossa, D. C., Babel, M. S., & Gupta, A. Das. (2010). Drought analysis in the Awash river basin, Ethiopia. *Water Resources Management*, *24*(7), 1441–1460. https://doi.org/https://10.1007/s11269-009-9508-0

Edwards, D. C. (1997). *Characteristics of 20th Century drought in the United States at multiple time scales.* AIR FORCE INST OF TECH WRIGHT-PATTERSON AFB OH. https://doi.org/http://hdl.handle.net/10217/170176

Eze, E., Okolo, C. C., & Negash, E. (2020). *Yield and yield-reduction in recent drought years in southern Tigray, northern Ethiopia: Implications on food security*.

FAO. (2002). *Major soils of the world land and water digital media series. Rome: Food and Agricultural Organization of the United Nations CD-ROM*.

Favre, A., El Adlouni, S., Perreault, L., Thiémonge, N., & Bobée, B. (2004). Multivariate hydrological frequency analysis using copulas. *Water Resources Research*, *40*(1). https://doi.org/https://doi.org/10.1029/2003WR002456

Fentaw, F., Hailu, D., Nigussie, A., & Melesse, A. M. (2018). Climate change impact on the hydrology of Tekeze Basin, Ethiopia: projection of rainfall-runoff for future water resources planning. *Water Conservation Science and Engineering*, *3*(4), 267–278. https://doi.org/https://doi.org/10.1007/s41101-018-0057-3

Gao, P., Mu, X.-M., Wang, F., & Li, R. (2011). Changes in streamflow and sediment discharge and the response to human activities in the middle reaches of the Yellow River. *Hydrology and Earth System Sciences*, *15*(1), 1.

Gebrehiwot, T., van der Veen, A., & Maathuis, B. (2011). Spatial and temporal assessment of drought in the Northern highlands of Ethiopia. *International Journal of Applied Earth Observation and Geoinformation*, *13*(3), 309–321. https://doi.org/https://doi.org/10.1016/j.jag.2010.12.002

Gebremicael, T. G., Mohamed, Y. A., Zaag, P. V., & Hagos, E. Y. (2017). Temporal and spatial changes of rainfall and streamflow in the Upper Tekezē-Atbara river basin, Ethiopia. *Hydrology and Earth System Sciences*, *21*(4), 2127–2142. https://doi.org/10.5194/hess-21-2127-2017

Ghafori, V., Sedghi, H., Sharifan, R. A., & Nazemosadat, S. M. J. (2019). Regional frequency analysis of droughts using copula functions (Case study: Part of semiarid climate of Fars Province, Iran). *Iranian Journal of Science and Technology, Transactions of Civil Engineering*, 1–13. https://doi.org/https://doi.org/10.1007/s40996-019-00297-5

Gidey, E., Dikinya, O., Sebego, R., Segosebe, E., & Zenebe, A. (2018). Predictions of future meteorological drought hazard (~ 2070) under the representative concentration path (RCP) 4.5 climate change scenarios in Raya, Northern Ethiopia. *Modeling Earth Systems and Environment*, *4*(2), 475–488. https://doi.org/https://doi.org/10.1007/s40808-018-0453-x

Girma, A. (2017). *R software script for meteorological data gap filling using the delta approach*.

Hao, C., Zhang, J., & Yao, F. (2017). Multivariate drought frequency estimation using copula method in Southwest China. *Theoretical and Applied Climatology*, *127*(3–4), 977–991.

Hao, Z., & AghaKouchak, A. (2013). Multivariate standardized drought index: a parametric multi-index model. *Advances in Water Resources*, *57*, 12–18. https://doi.org/https://doi.org/10.1016/j.advwatres.2013.03.009

Hastings, C. (1955). Approximations for Digital Computers (Princeton: University). *Princeton, NJ*.

Kao, S.-C., & Govindaraju, R. S. (2010). A copula-based joint deficit index for droughts. *Journal of Hydrology*, *380*(1–2), 121–134.

Katsanos, D., Retalis, A., & Michaelides, S. (2016). Validation of a high-resolution precipitation database (CHIRPS) over Cyprus for a 30-year period. *Atmospheric Research*, *169*, 459–464. https://doi.org/https://doi.org/10.1016/j.atmosres.2015.05.015

Kendall, M. G. (1975). Rank correlation measures. *Charles Griffin, London*, *202*, 15.

Kwon, M., Kwon, H., & Han, D. (2019). Spatio-temporal drought patterns of multiple drought indices based on precipitation and soil moisture: A case study in South Korea. *International Journal of Climatology*, *39*(12), 4669–4687. https://doi.org/https://doi.org/10.1002/joc.6094

Li, C., Singh, V. P., & Mishra, A. K. (2013). A bivariate mixed distribution with a heavy-tailed component and its application to single-site daily rainfall simulation. *Water Resources Research*, *49*(2), 767–789. https://doi.org/https://doi.org/10.1002/wrcr.20063

Li, W., Yi, X., Hou, M., Chen, H., & Chen, Z. (2012). Standardized precipitation evapotranspiration index shows drought trends in China. *Zhongguo Shengtai Nongye Xuebao/Chinese Journal of Eco-Agriculture*, *20*(5), 643–649. https://doi.org/10.3724/SP.J.1011.2012.00643

Liou, Y.-A., & Mulualem, G. M. (2019). Spatio–temporal assessment of drought in ethiopia and the impact of recent intense droughts. *Remote Sensing*, *11*(15), 1828. https://doi.org/https://doi.org/10.3390/rs11151828

Mann, H. B. (1945). Nonparametric tests against trend. *Econometrica: Journal of the Econometric Society*, 245–259.

Mirakbari, M., Ganji, A., & Fallah, S. R. (2010). Regional bivariate frequency analysis of meteorological droughts. *Journal of Hydrologic Engineering*, *15*(12), 985–1000.

Nash, J. E., & Sutcliffe, J. V. (1970). River flow forecasting through conceptual models part I—A discussion of principles. *Journal of Hydrology*, *10*(3), 282–290. https://doi.org/https://10.1016/0022- 1694(70)90255-6

Nicholson, S. E. (2000). The nature of rainfall variability over Africa on time scales of decades to millenia. *Global and Planetary Change*, *26*(1–3), 137–158.

Saadat, S., Khalili, D., Kamgar-Haghighi, A. A., & Zand-Parsa, S. (2013). Investigation of spatio-temporal patterns of seasonal streamflow droughts in a semi-arid region. *Natural Hazards*, *69*(3), 1697–1720.

Sadegh, M., Ragno, E., & AghaKouchak, A. (2017). Multivariate C opula A nalysis T oolbox (MvCAT): describing dependence and underlying uncertainty using a B ayesian framework. *Water Resources Research*, *53*(6), 5166–5183.

Schwarz, G. (1978). Estimating the dimension of a model. *The Annals of Statistics*, *6*(2), 461–464.

Shekhar, A., & Shapiro, C. A. (2019). What do meteorological indices tell us about a long-term tillage study? *Soil and Tillage Research*, *193*, 161–170. https://doi.org/https://doi.org/10.1016/j.still.2019.06.004

Shepard, D. (1968). A two-dimensional interpolation function for irregularly-spaced data. *Proceedings of the 1968 23rd ACM National Conference*, 517–524.

Shiau, J. T. (2006). Fitting drought duration and severity with two-dimensional copulas. *Water Resources Management*, *20*(5), 795–815. https://doi.org/https://doi.org/10.1007/s11269-005-9008-9

Shukla, S., McNally, A., Husak, G., & Funk, C. (2014). A seasonal agricultural drought forecast system for food-insecure regions of East Africa. *Hydrology and Earth System Sciences*, *18*(10), 3907–3921. https://doi.org/https://doi.org/10.5194/hess-18-3907-2014

Sklar, M. (1959). Fonctions de repartition an dimensions et leurs marges. *Publ. Inst. Statist. Univ. Paris*, *8*, 229–231.

Song, S., & Singh, V. P. (2010). Frequency analysis of droughts using the Plackett copula and parameter estimation by genetic algorithm. *Stochastic Environmental Research and Risk Assessment*, *24*(5), 783–805. https://doi.org/https://doi.org/10.1007/s00477-010-0364-5

Sousa, P. M., Trigo, R. M., Aizpurua, P., Nieto, R., Gimeno, L., & Garcia-Herrera, R. (2011). Trends and extremes of drought indices throughout the 20th century in the Mediterranean. *Natural Hazards and Earth System Sciences*, *11*(1), 33–51.

Temam, D., Uddameri, V., Mohammadi, G., Hernandez, E. A., & Ekwaro-Osire, S. (2019). Long-term drought trends in Ethiopia with implications for dryland agriculture. *Water*, *11*(12), 2571. https://doi.org/https://doi.org/10.3390/w11122571

Thom, Herbert C S. (1951). A frequency distribution for precipitation. *Bulletin of the American Meteorological Society*, *32*(10), 397.

Thom, Herbert Conrad Schlueter. (1966). *Some methods of climatological analysis*.

Vaziri, H., Karami, H., Mousavi, S.-F., & Hadiani, M. (2018). Analysis of hydrological drought characteristics using copula function approach. *Paddy and Water Environment*, *16*(1), 153–161. https://doi.org/https://doi.org/10.1007/s10333-017-0626-7

Wilhite, D. A., & Vanyarkho, O. V. (2000). Drought: Pervasive impacts of a creeping phenomenon. In D. A. Wilhite (Ed.), *Drought: A Global Assessment* (1st ed., pp. 245–255). Drought – National Drought Mitigation Center.

http://digitalcommons.unl.edu/droughtfacpub/71

WMO. (2009). *Guide to hydrological practices, volume II: Management of water resources and application of hydrological practices*. World Meteorological Organization Geneva, Switzerland.

Yisehak, B., & Zenebe, A. (2020). Modeling multivariate standardized drought index based on the drought information from precipitation and runoff : a case study of Hare watershed of Southern Ethiopian Rift Valley Basin. *Modeling Earth Systems and Environment*, *6*(0123456789). https://doi.org/https://doi.org/10.1007/s40808-020-00923-6

Zhang, Q., Qi, T., Singh, V. P., Chen, Y. D., & Xiao, M. (2015). Regional frequency analysis of droughts in China: a multivariate perspective. *Water Resources Management*, *29*(6), 1767–1787. https://doi.org/https://doi.org/10.1007/s11269-014-0910-x

Zhao, C., Cui, Y., Zhou, X., & Wang, Y. (2016). Evaluation of performance of different methods in detecting abrupt climate changes. *Discrete Dynamics in Nature and Society*, *2016*.

Figures

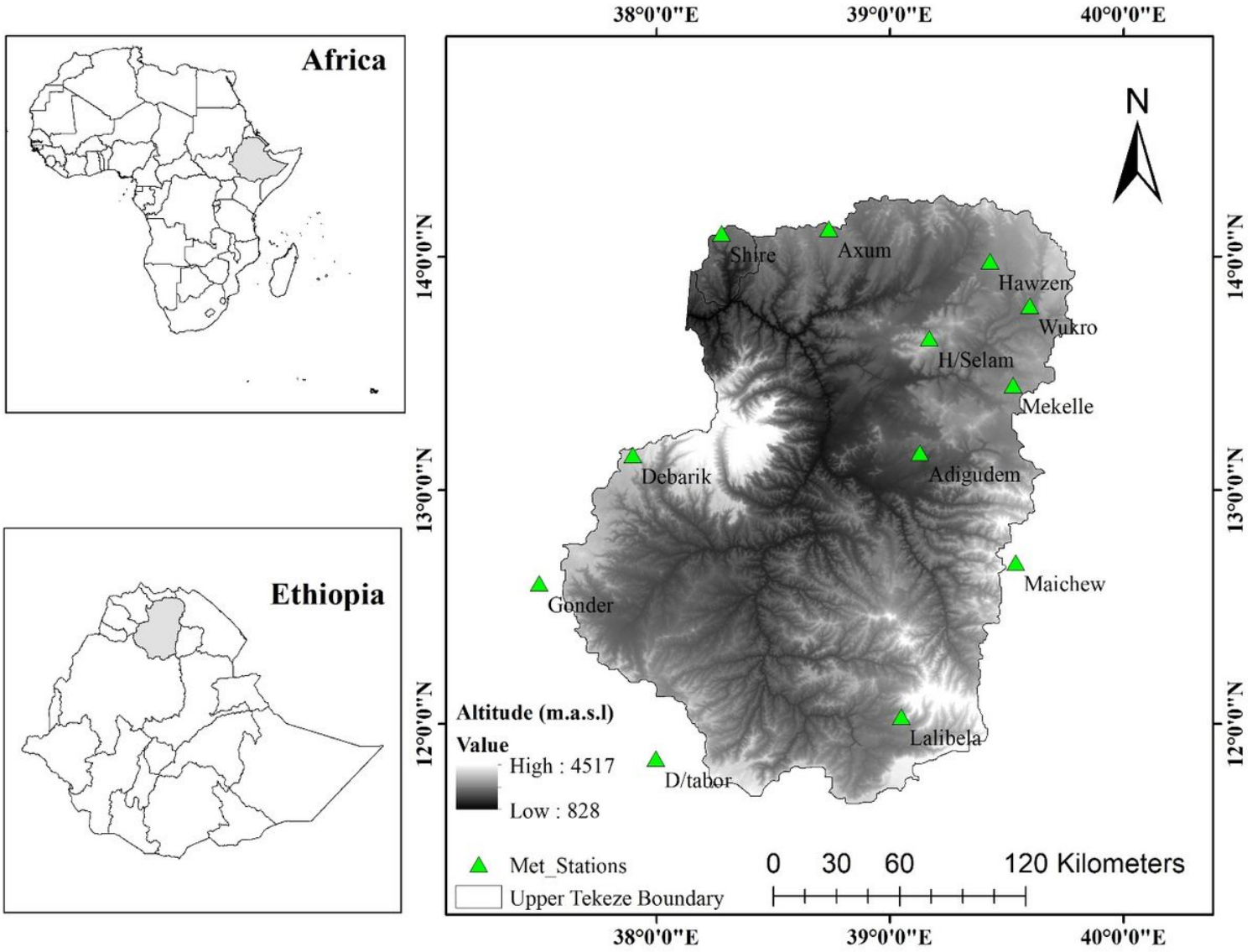

Figure 1

Location, distribution of rainfall stations, elevation in meter, and Upper Tekezr River boundary, based on a digital elevation model of Shuttle Radar Topographic Mission 30m in Upper Tekeze River Basin Northern Ethiopia

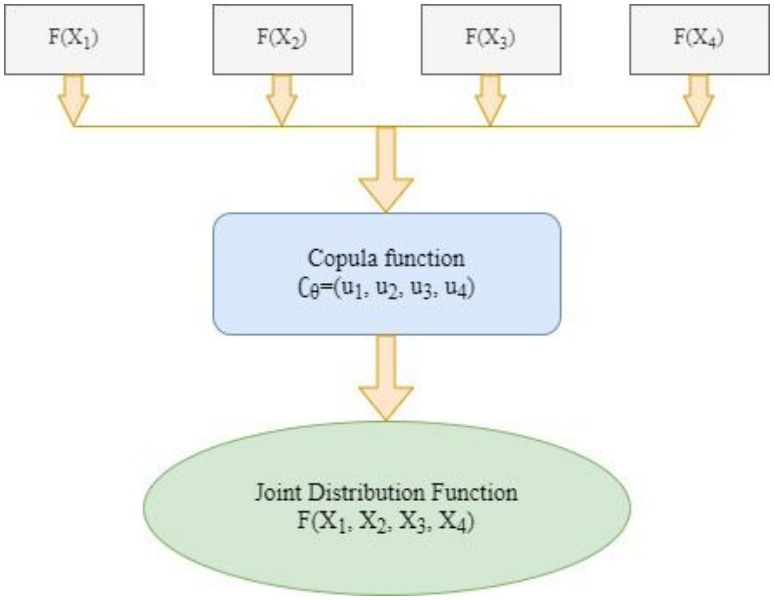

Figure 2

Schematic workflow for Copula model

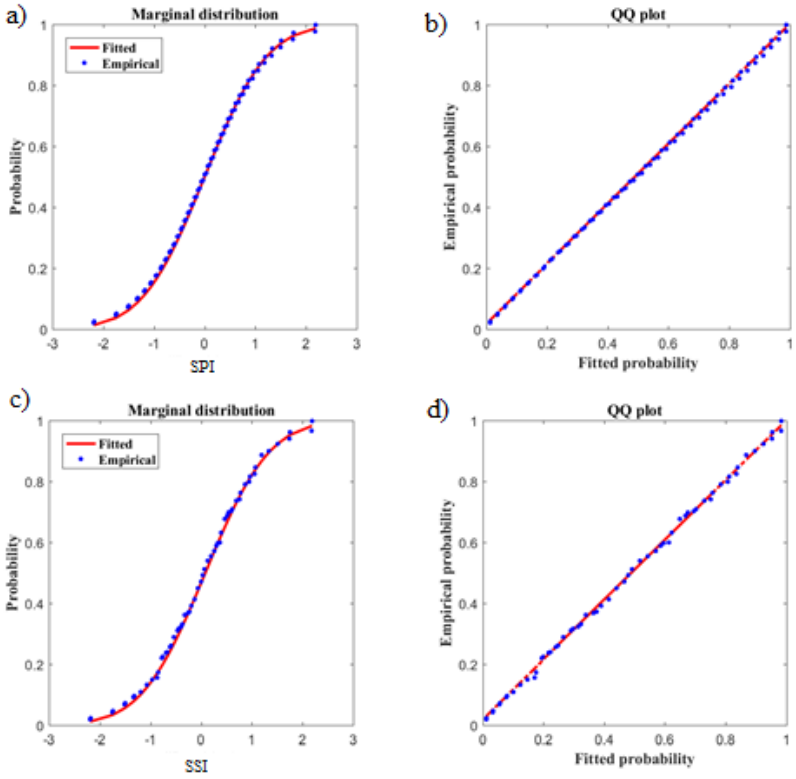

Figure 3

Empirical and fitted probability distributions: a) standardized precipitation index (SPI), b) quantile-quantile (QQ) plot of empirical probability versus fitted probability of SPI and c) standardized soil moisture (SSI), d) quantile-quantile (QQ) plot of empirical probability versus fitted probability of SSI. The red solid lines present the fitted probabilities and the blue dots show empirical probability.

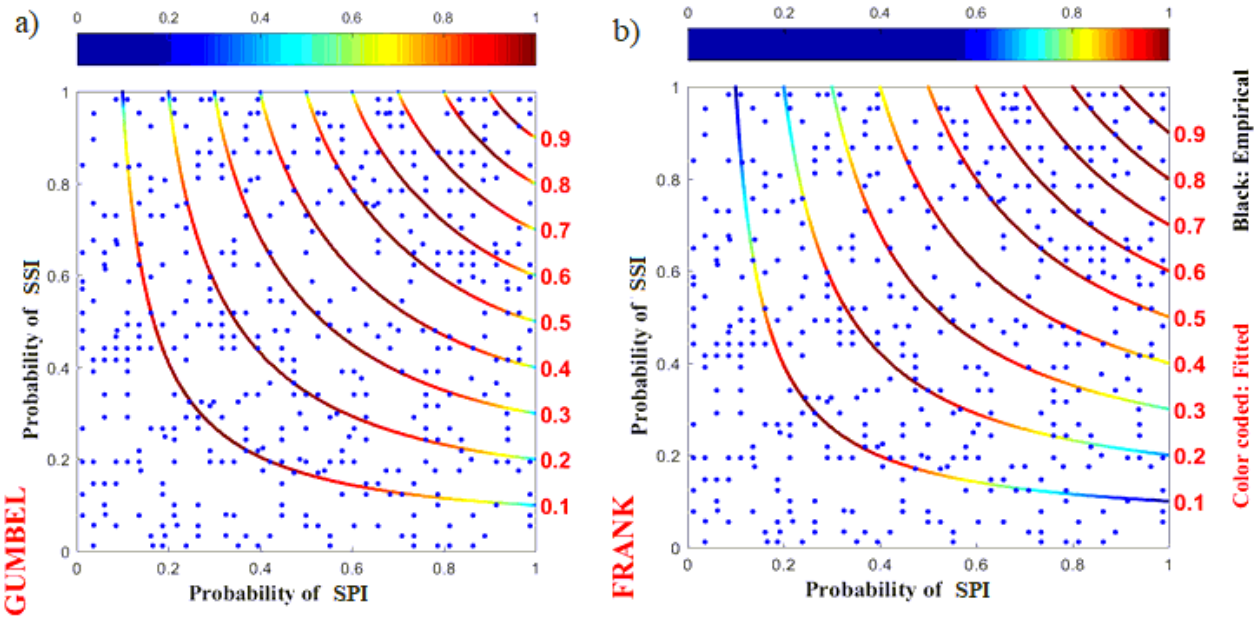

Figure 4

Dependent structure of standardized precipitation index (SPI) and standardized soil moisture index (SSI) in Upper Tekeze River Basin. The curved lines present the copula isolines and the blue dots show observed data. Gumbel copula is used for 3- and 6-month drought timescales (a), whereas the Frank copula is used to model dependence of SPI and SSI for 12-month drought timescale (b), from 1982 to 2020.

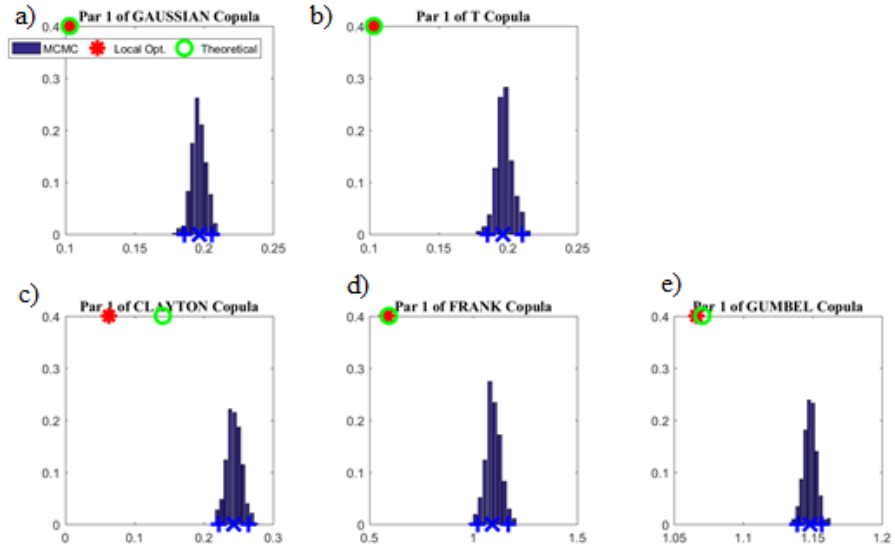

Figure 5

Posterior distribution of a) Gaussian, b) T-copula, c) Clayton, d) Frank, and e) Gumbel derived by the Markov Chain Monte Carlo (MCMC) simulation within a Bayesian framework. Red strikes on the top of each figure show copula parameter value derived by local optimization approach, whereas the blue bins are the MCMC-derived parameters and the blue cross shows the maximum likelihood parameter of the MCMC.

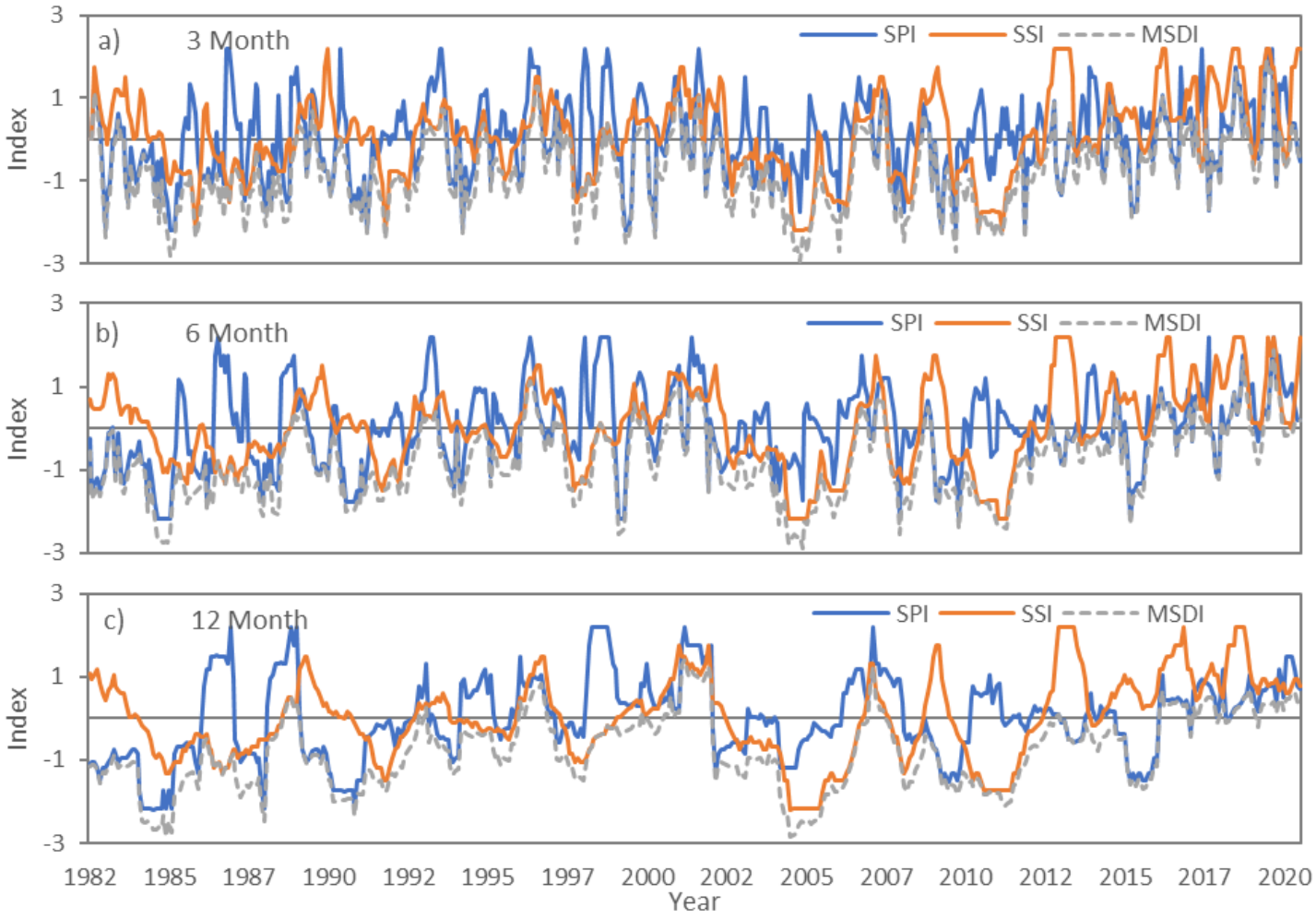

Figure 6

The temporal variability of meteorological drought for 3-month, 6-month, and 12-month SPI, SSI, and MSDI during 1982-2020 for the Upper Tekeze River Basin, Northern Ethiopia

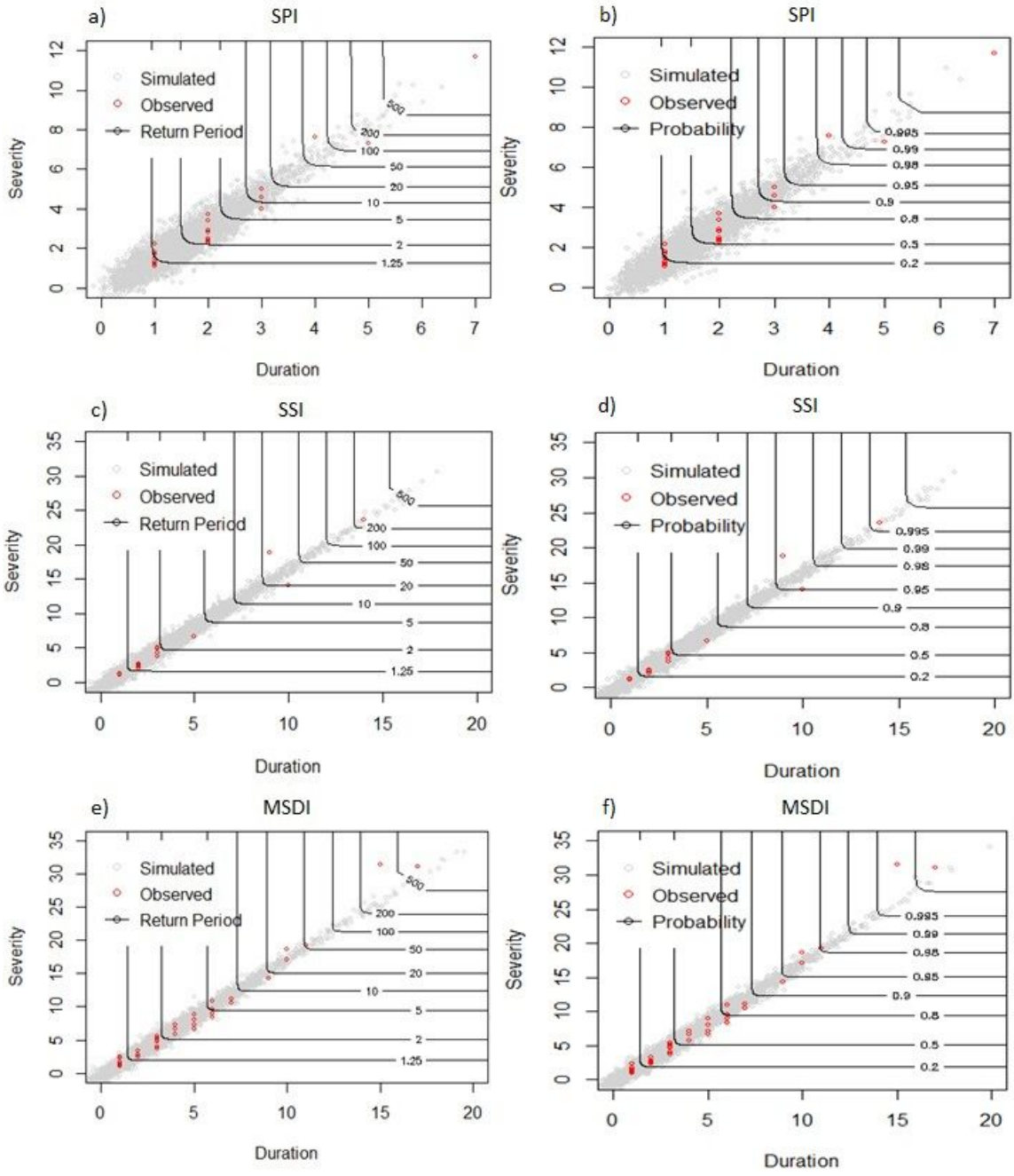

Figure 7

Joint return period and probability of non-exceedance drought severity and duration (D>d or S>s) for a 3-month drought timescale during 1982-2020 in the Upper Tekeze River Basin, Northern Ethiopia. Standardized precipitation index (SPI)(a-b), Standardized soil moisture index (SSI)(c-d), Multivariate standardized drought index (MSDI)(e-f). The red circles on each figure show observed value, whereas the light gray circles on each figure show simulated value, and the contour lines on each Figure (a, c, and e) show joint return period and Figure (b, d, and f) shows the probability of non-exceedance.

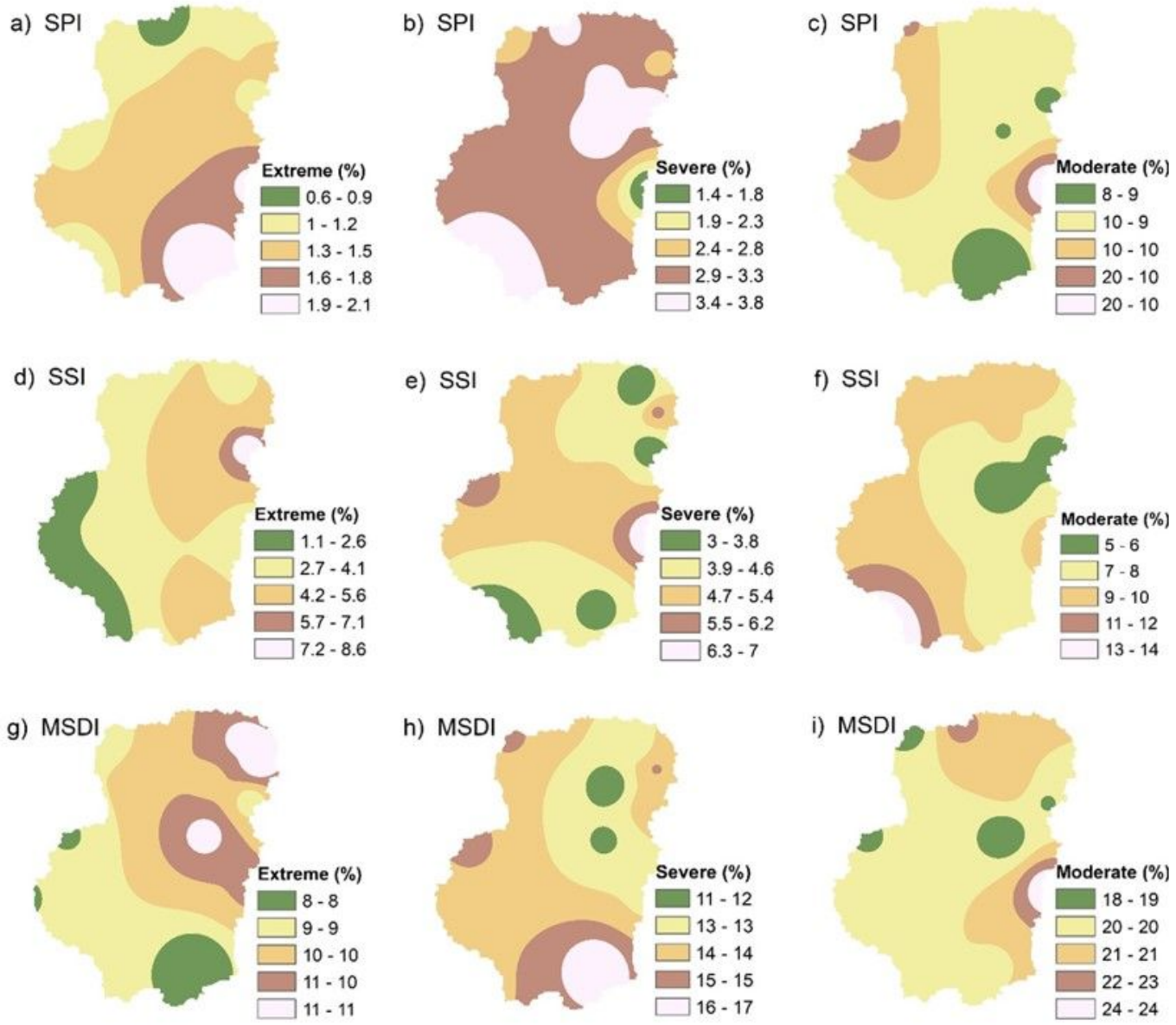

Figure 8

Based on 3-month SPI, SSI, and MSDI, the percentage occurrence of extreme, severe, and moderate drought during 1982-2020 in Upper Tekeze River Basin (UTRB) Northern Ethiopia